Progress In Electromagnetics Research B, Vol. 17, 293–308, 2009

ON THE IMPACT OF MUTUAL COUPLING EFFECTS ON THE PSL PERFORMANCES OF ADS THINNED ARRAYS

G. Oliveri, L. Manica, and A. Massa

Department of Information and Communication Technologies
University of Trento
Via Sommarive 14, Trento 38050, Italy

Abstract—In this paper, the performances of thinned arrays based on Almost Difference Sets are analyzed in the presence of mutual coupling effects. The geometry under test is composed by thin dipole elements and the arising mutual interactions are modeled by means of the induced EMF method. To assess the robustness of the *ADS*-based thinning technique also in such a non-ideal case, an extensive numerical analysis is carried out by considering several test cases characterized by different aperture sizes, lattice spacings, and thinning factors. The obtained results show that the peak sidelobe estimators deduced in the ideal case still keep their validity although, as expected, a deterioration usually arises due to the mutual coupling.

1. INTRODUCTION

Large antenna arrays providing low sidelobes are of great interest in several applications including radar, microwave imaging, remote sensing, radio astronomy, satellite and ground communications [1]. In such a framework, filled arrangements are characterized by very high costs, weight, and power consumption and usually require complex feeding network. On the other hand, removing some elements from the array generally increases the peak sidelobe level (PSL) of the radiated pattern. As a consequence, suitable thinning techniques have been introduced to reduce the array elements while obtaining low PSL values [2] and several approaches have been proposed. Randomly thinned arrays have provided predictable results [3] and improved PSLs with respect to deterministic techniques [4]. Stochastic approaches based on genetic algorithms (GAs) [2, 5–13], simulated

Corresponding author: A. Massa (andrea.massa@ing.unitn.it).

annealing (SA) [14, 15], pattern search [16], and particle swarm optimizers (PSOs) [17, 18] have been successfully applied to reach enhanced PSL performances although their computational complexity rapidly grows with the aperture size and no predictors are available to *a-priori* estimate their performances. On the contrary, thinning techniques exploiting difference sets (DSs) [19] allow one to obtain low PSLs and predictable results in a very effective fashion. Unfortunately, only a limited set of thinning factors and aperture sizes [19] can be dealt with because of the reduced set of available sequences. In order to enlarge the set of admissible array configurations almost difference sets (ADSs) [20] or their subsets [21, 22] have been recently employed to thin linear geometries. In [23], it has been shown that the PSL of ADS-based *ideal arrays*[†] is (a) *a-priori* bounded, (b) comparable to that of DS-based designs, and (c) significantly better than that of random arrangements [23]. However, it is worth noticing that analytic bounds for the PSL behavior are available only for *ideal arrays*, while neither *a-priori* estimates exist nor simple extensions of the ADS array theory have been deduced in the presence of non-ideal radiators when mutual coupling (MC) effects between the array elements take place.

In this paper, the performances of ADS-based linear thinned arrays are analyzed in the presence of MC effects to assess the reliability of the PSL bounds yielded in [23]. The paper is not aimed at defining an optimal synthesis strategy for non-ideal arrays, but to provide to the antenna designer an indication on the robustness of the ADS-based thinning technique. Towards this end, the paper is organized as follows. In Sec. 2, the ADS-based thinning approach is summarized and some details on the considered MC model are provided. Sec. 3 is concerned with an extensive numerical analysis devoted to show the dependence of the PSL performances of non-ideal arrays on the aperture size, the inter-element spacing, and the thinning factor. Finally, some conclusions are drawn (Sec. 4).

2. MATHEMATICAL FORMULATION

Let us consider a one-dimensional regular lattice of N positions spaced by d wavelengths (λ being the free-space wavelength). The power pattern radiated from the linear thinned array defined over such a lattice is equal to [1]

$$PP(u) = \left| \sum_{n=0}^{N-1} w(n) \exp\left(j2\pi n d u\right) \right|^2 \tag{1}$$

[†] In this paper, the term *ideal array* indicates an array of identical isotropic elements without mutual coupling effects.

where $u = \sin(\theta)$ and $w(n) \in \{0, 1\}$ is the excitation coefficient of the array element located at the n-th location of the lattice whose binary value is defined according to the *ADS*-based guideline [23]:

$$w(n) = \begin{cases} 1 & \text{if } n \in \underline{\mathbf{D}} \\ 0 & \text{if } n \notin \underline{\mathbf{D}}. \end{cases} \tag{2}$$

$\underline{\mathbf{D}} \triangleq \left\{ d_k \in \mathbb{Z}^N,\, d_h \neq d_l,\, k, l, h = 0, \ldots, K-1 \right\}$ being a (N, K, Λ, t)-*ADS*. More in detail, an *ADS* is a K-subset of $\mathbb{Z}^N$ characterized by a three-valued cyclic autocorrelation [24, 25]

$$\begin{aligned} A_w\left(\underline{\mathbf{D}}\right) &= \sum_{n=0}^{N} w\left(n\right) w\left[\left(n+\tau\right) mod\, N\right] \\ &= \begin{cases} K & \tau = 0 \\ \Lambda & \text{for } t \text{ values of } \tau \in [1, N-1] \\ \Lambda + 1 & \text{elsewhere} \end{cases} . \end{aligned} \tag{3}$$

As an example, let us consider the $(16, 8, 3, 4)$-*ADS* in [20], $\underline{\mathbf{D}}_1 \triangleq \{2, 3, 4, 5, 7, 12, 14, 15\}$, and the corresponding arrangement $\mathbf{W}\left(\underline{\mathbf{D}}_1\right) = \{0\,0\,1\,1\,1\,1\,0\,1\,0\,0\,0\,0\,1\,0\,1\,1\}$ whose n-th entry is equal to $w\left(n\right)$, $n = 0, \ldots, N-1$. In this case, $A_w\left(\underline{\mathbf{D}}\right)$ results

$$A_w\left(\underline{\mathbf{D}}\right) = \begin{cases} 8 & \tau = 0 \\ 3 & \tau = 4, 6, 10, 12 \\ 4 & \tau = 1, 2, 3, 5, 7, 8, 9, 11, 13, 14, 15 \end{cases} .$$

The exploitation of the *ADS* properties guarantees that the arising one-dimensional ideal array satisfies the following set of inequalities [23]

$$PSL_{\mathrm{MIN}} \leq PSL_{DW} \leq PSL_{opt} \leq PSL_{UP} \leq PSL_{\mathrm{MAX}} \tag{4}$$

where

$$\begin{aligned} PSL_{\mathrm{MAX}} &= E\{\Phi_N^{\min}\} \frac{K - \Lambda - 1 + \sqrt{t(N-t)}}{(N-1)\Lambda + K - 1 + N - t}, \\ PSL_{\mathrm{MIN}} &= \frac{K - \Lambda - 1 - \sqrt{\frac{t(N-t)}{(N-1)}}}{(N-1)\Lambda + K - 1 + N - t}, \quad PSL_{UP} = \xi E\{\Phi_N^{\min}\}, \\ PSL_{DW} &= \xi, \quad E\{\Phi_N^{\min}\} \approx 0.8488 + 1.128 \log_{10} N. \end{aligned}$$

Moreover, $PSL_{opt} = \min_\sigma\{PSL(\underline{\mathbf{D}}^{(\sigma)})\}$, $\underline{\mathbf{D}}^{(\sigma)}$ being the cyclic shift of the sequence $\underline{\mathbf{D}}$, $\underline{\mathbf{D}}^{(\sigma)} \triangleq \{d_k^{(\sigma)} \in \mathbb{Z}^N,\, k = 1, \ldots, K : d_k^{(\sigma)} = (d_k + \sigma) mod\, N\}$, and $PSL(\underline{\mathbf{D}}^{(\sigma)}) \triangleq \frac{\max_{u \notin R_m}\{PP(u)\}}{PP(0)}$. As regards to R_m, it indicates the mainlobe region [19] defined as $R_m \triangleq \{-U_M \leq u \leq U_M,\, U_M = \frac{1}{2Nd\sqrt{\xi}}\}$ where $\xi \triangleq \frac{1}{K^2} \max_l\{PP(\frac{nl}{Nd})\}$ [23].

The inequality in (4) holds true for any *ADS*-based ideal arrangement provided that N is sufficiently large [23] and d is below 1 (e.g., $d \leq 0.85$) since when $d \to 1$ a grating lobe necessarily appears. On the other hand, it should be observed that no indications are available or can be envisaged starting from (4) on the behavior of *ADS*-based arrays in the presence of *MC* effects. As a matter of fact, *MC* cannot be analytically taken into account to easily derive an extended version of (4) since (3) holds true only in ideal conditions. Therefore, a numerical analysis is mandatory to investigate on the reliability and the robustness of the *PSL* bounds derived in [23]. Towards this end, the mutual coupling model presented in [26] is adopted. The peak sidelobe level of *ADS* arrays in the presence of mutual coupling is defined as $PSL^{MC}(\underline{\mathbf{D}}^{(\sigma)}) \triangleq \frac{\max_{u \notin R_m}\{PP^{MC}(u)\}}{PP^{MC}(0)}$ where $PP^{MC}(u) = |\sum_{n=0}^{N-1} w^{MC}(n) \exp(j2\pi ndu)|^2$. The mutual coupling effects are modeled through the perturbed array vector $\mathbf{W}^{MC}(\underline{\mathbf{D}})$ [26] given by

$$\mathbf{W}^{MC}(\underline{\mathbf{D}}) = Z_L (\mathbf{Z} + Z_L \mathbf{I})^{-1} \mathbf{W}(\underline{\mathbf{D}}) \tag{5}$$

where Z_L is the load impedance at each element of the array and $\mathbf{Z}$ is the mutual impedance matrix of $(N-1) \times (N-1)$ entries computed through the induced EMF method [1] once the array elements are chosen.

3. NUMERICAL ANALYSIS

In this section, the performances of *ADS*-based arrays in the presence of mutual coupling effects are discussed to numerically assess whether the ideal *PSL* bounds are still valid when non-ideal radiators are taken into account. Towards this end, dipole elements of length $l = \frac{\lambda}{2}$ and radius $\rho = 5 \times 10^{-4}$ (in wavelength) have been considered. Accordingly, the dipole self-impedance turns out to be equal to $Z_{ii} \approx 73.12 + j\,42.2\,[\Omega]$, $i = 0, \ldots, N-1$, [1] while the mutual impedances assume the following expression [1]

$$Z_{ij} = j\frac{\eta_0}{4\pi} \int_{-\frac{\lambda}{4}}^{\frac{\lambda}{4}} \sin\left[k\left(\frac{\lambda}{4} - |z|\right)\right]\left[\frac{e^{-jkR_+}}{R_+} + \frac{e^{-jkR_-}}{R_-}\right] dz,\ i \neq j,\ i,j \in [0, N-1],$$

η_0 and k being the free-space impedance and the wavenumber, respectively. Moreover, $R_\pm = \sqrt{\delta_{ij}^2 + (z \pm \frac{\lambda}{4})^2}$ and δ_{ij} is the distance between the elements i and j.

The first experiment is aimed at analyzing the behavior of the *PSL* of *ADS* sequences with and without mutual coupling in

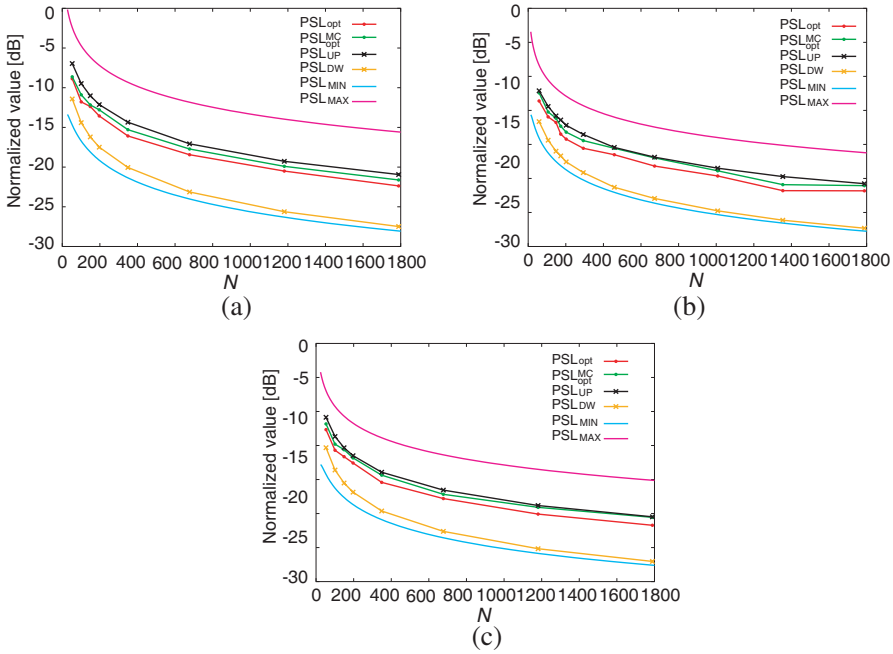

Figure 1. $[d = 0.5]$ — Plots of the PSL of ADS-based arrays with and without MC versus N when (a) $\nu = 0.25$, (b) $\nu = 0.5$, and (c) $\nu = 0.75$.

correspondence with a half-wavelength lattice ($d = \frac{\lambda}{2}$) and different number of elements. Fig. 1 gives the plot of the optimal PSL value for different values of the thinning factor, $\nu \triangleq \frac{K}{N}$. As it can be observed, the PSLs of ADS arrays affected by mutual coupling still satisfy (4) whatever the indexes N and ν ($PSL_{DW} \leq PSL_{opt}^{MC} \leq PSL_{UP}$) although their values increase and usually result closer to the upper bound threshold PSL_{UP} as ν grows [Fig. 1(c) vs. Fig. 1(a)]. As a matter of fact, the impact of mutual coupling effects reduces when the average spacing between adjacent array elements, $d_{av} \approx \frac{d}{\nu}$, enlarges (i.e., $\nu \to 0$). Such an event is further confirmed by the behavior of the peak sidelobe level versus σ as shown in Fig. 2 ($N = 149$). As expected, the optimal shift

$$\sigma_{opt} = \arg \left\{ \max_{\sigma \in [0, N-1]} \left[PSL \left(\underline{\mathbf{D}}^{(\sigma)} \right) \right] \right\}$$

is kept unaltered when $\nu = 0.25$ [Fig. 2(a)] since the mutual coupling effects modify only to a small extent the power pattern of the ideal

array [Fig. 2(d)]. Otherwise, $\sigma_{opt} \neq \sigma_{opt}^{MC}$ when $\nu = 0.5$ [Fig. 2(b)] and $\nu = 0.75$ [Fig. 2(c)] since the optimal patterns significantly differ. Similar conclusions hold true also when dealing with larger apertures as shown in Fig. 3 ($N = 1789$).

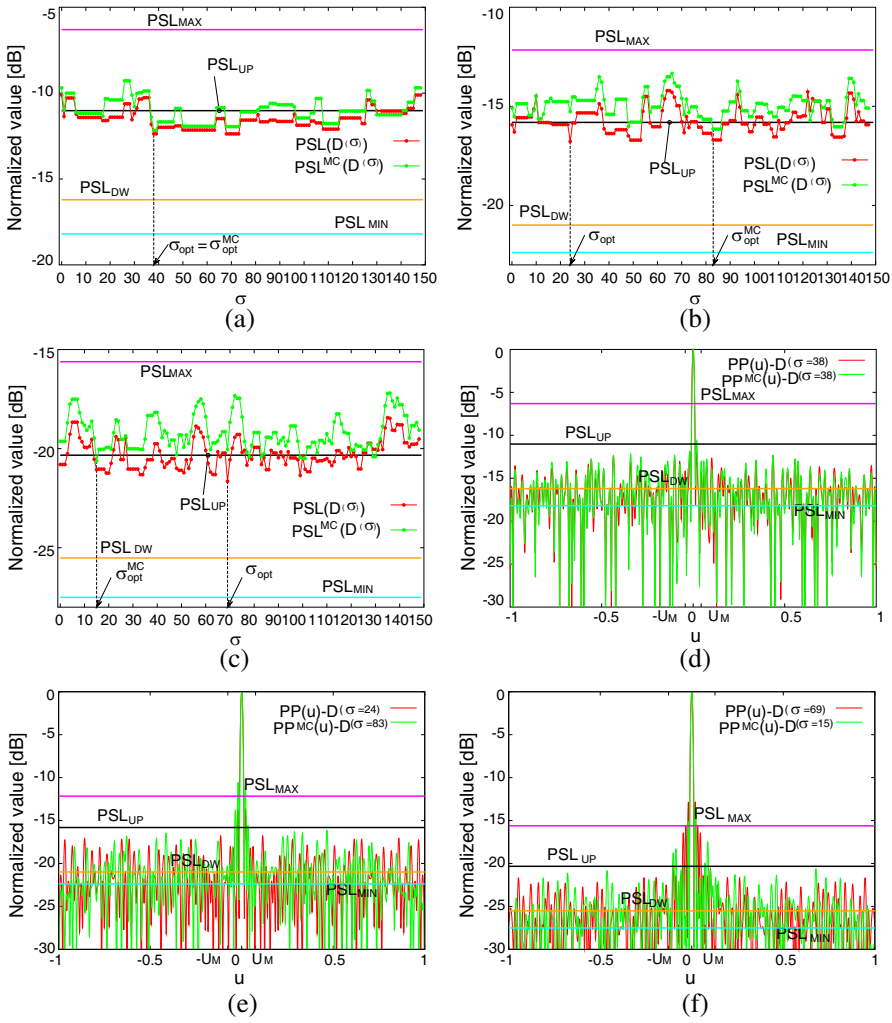

Figure 2. [$N = 148$, $d = 0.5$] — Plots of PSL ($\underline{\mathbf{D}}^{(\sigma)}$) and PSL_{MC} ($\underline{\mathbf{D}}^{(\sigma)}$) versus σ (a)–(c) and beam patterns generated by the optimal shifts σ_{opt} and σ_{opt}^{MC} (d)–(f) when $\nu = 0.25$ (a)(d), $\nu = 0.5$ (b)(e), and $\nu = 0.75$ (c)(f).

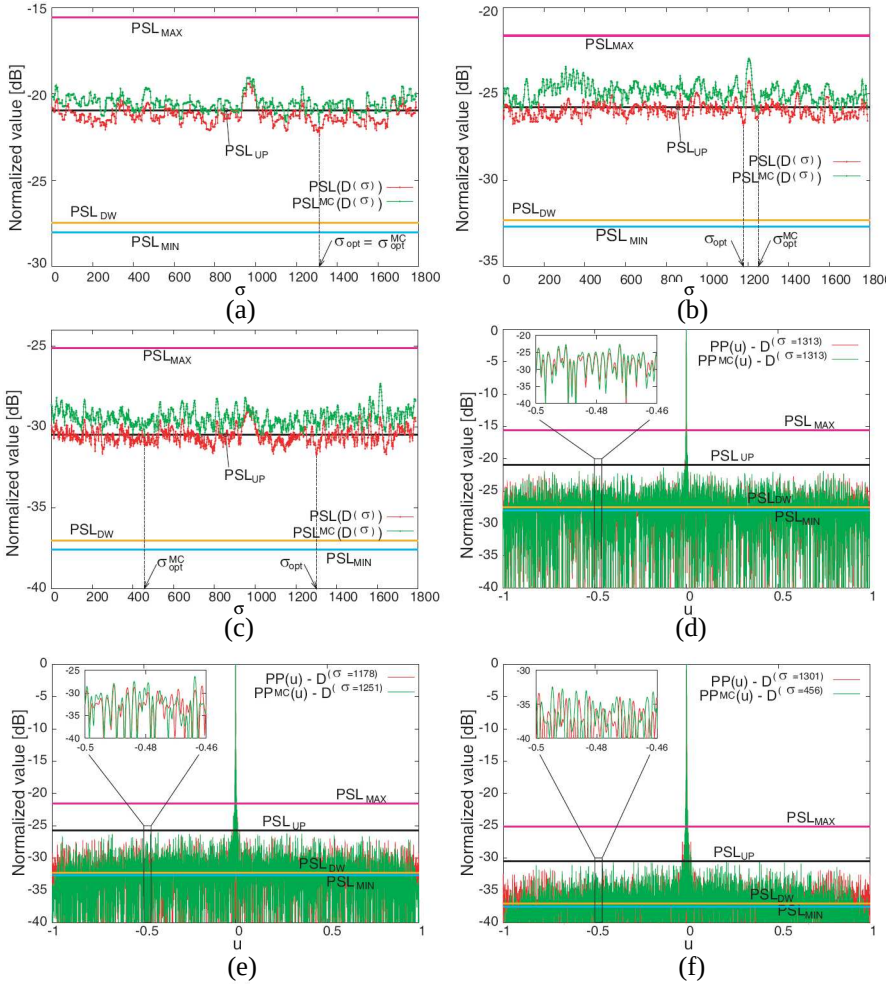

Figure 3. $[N = 1789,\ d = 0.5]$ — Plots of PSL ($\underline{\mathbf{D}}^{(\sigma)}$) and PSL_{MC} ($\underline{\mathbf{D}}^{(\sigma)}$) versus σ (a)–(c) and beam patterns generated by the optimal shifts σ_{opt} and σ_{opt}^{MC} (d)–(f) when $\nu = 0.25$ (a)(d), $\nu = 0.5$ (b)(e), and $\nu = 0.75$ (c)(f).

It is also worth noticing that, despite the MC and whatever the dimension of the array lattice, more than one shift presents a PSL within the ideal bounds as for ideal arrays. However, the number of the optimal shifts reduces as pointed out in Fig. 4 where the percentages of optimal shifts with, Ω^{MC}, and without mutual coupling, Ω, versus the aperture size are reported.

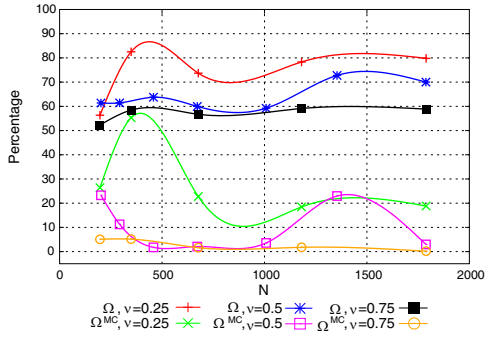

Figure 4. $[d = 0.5]$— Plots of Ω and Ω^{MC} versus N for different thinning factors, $\nu = 0.25, 0.5, 0.75$.

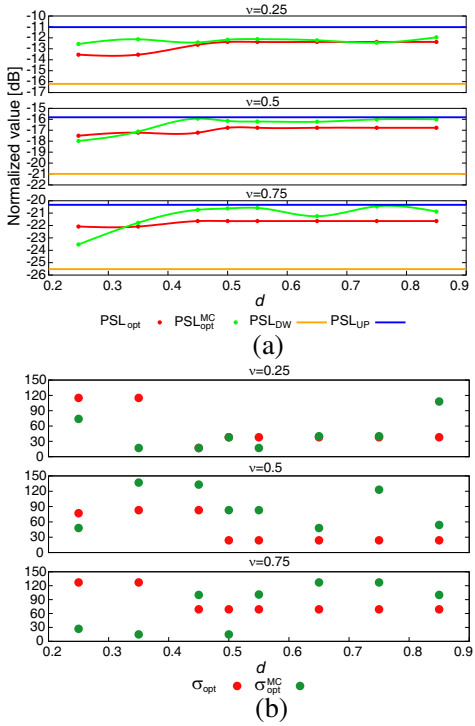

Figure 5. $[N = 148]$ — Plots of PSL_{opt} (a) and shift number σ_{opt} (b) versus the inter-element distance d for different thinning indexes ($\nu = 0.25, 0.5, 0.75$).

Concerning lattices with $d \neq 0.5$, the second experiment deals with an array of $N \approx 150$ locations and it considers different ν values. Fig. 5(a) gives the plots of PSL_{opt} and PSL_{opt}^{MC} versus d. For completeness, the number of the corresponding optimal shift in the range $[0, N-1]$ is reported [Fig. 5(b)], as well. As it can be noticed, PSL_{opt}^{MC} still satisfies (4) [Fig. 5(a)] and its deviation from the ideal level turns out to be greater for larger thinning values, while negligible variations occur when $\nu = 0.25$ except for $d < 0.45$. In this latter case, the MC effects impact more significantly since the average inter-element distance turns out to be similar to that of filled configurations. On the other hand, Fig. 5(a) points out that usually $PSL_{opt} < PSL_{opt}^{MC}$ although there exists a small range of d values for which $PSL_{opt}^{MC} < PSL_{opt}$. Such a situation takes place when $\nu > 0.5$ in correspondence with a higher variability of the phases of the non-ideal weights when d reduces. Such a circumstance probably provides a constructive interference in minimizing the PSL value. For illustrative purposes, Fig. 6 shows a sample of the behavior of the

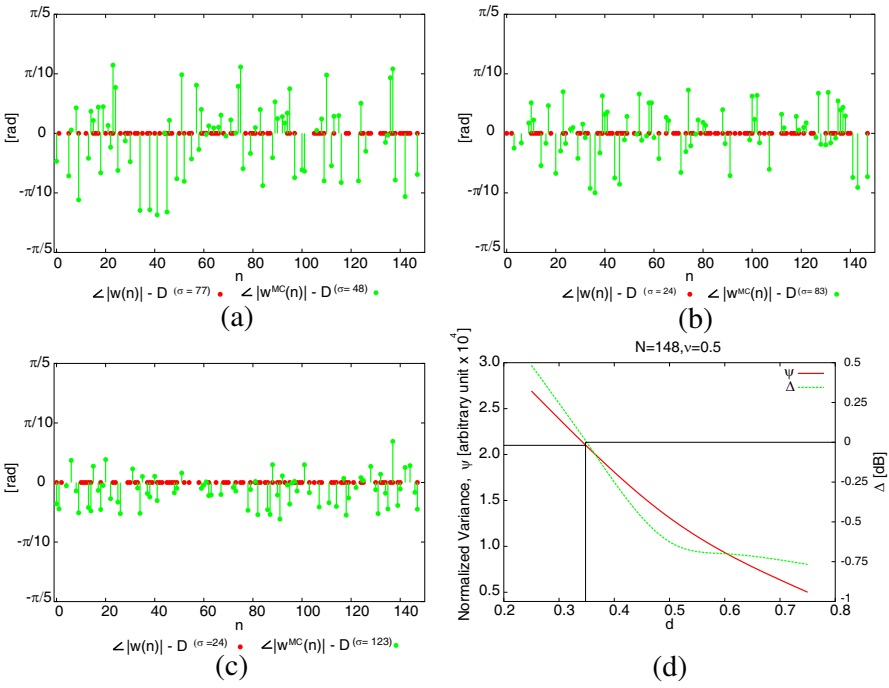

Figure 6. *ADS-based Array* (148, 74, 36, 37) [$N = 148$, $\nu = 0.5$] — Plots of the phases of the array weights when (a) $d = 0.25$, (b) $d = 0.5$, and (c) $d = 0.75$. Normalized variance Ψ and Δ value versus d (d).

phases of the coefficients $w^{MC}(n)$, $n = 0, \ldots, N-1$, [Figs. 6(a)–6(c)] as well as the plot of the normalized variance $\psi \triangleq \frac{var_n\{\angle w^{MC}(n)\}}{N}$ and of $\Delta \triangleq PSL_{opt}^{MC} - PSL_{opt}$ [Fig. 6(d)] when $\nu = 0.5$ and for different lattice spacings.

As far as the optimal shift is concerned and unlike the ideal case, the value of σ_{opt}^{MC} continuously changes in non-ideal arrays whatever the lattice distribution [σ_{opt}^{MC} vs. σ_{opt} — Fig. 5(b)] since a change of

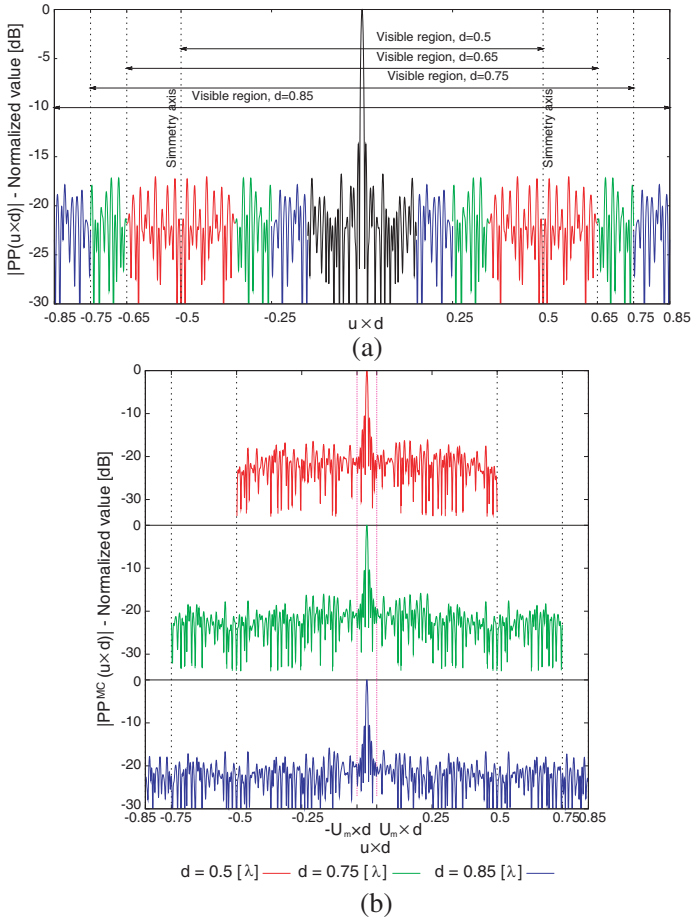

Figure 7. *ADS-based Array* (148, 74, 36, 37) [$N = 148$, $\nu = 0.5$] — Power patterns generated by (a) $\sigma = \sigma_{opt}|_{d=0.5} = 24$ and (b) $\sigma = \sigma_{opt}^{MC}|_{d=0.5} = 83$ in correspondence with different values of d.

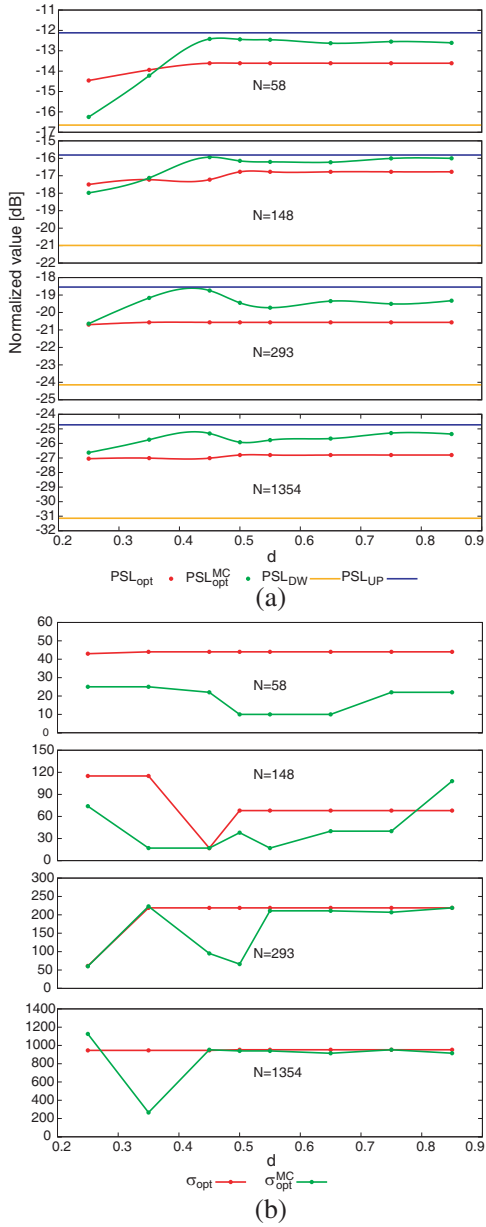

Figure 8. $[\nu = 0.5]$ — Plots of PSL_{opt} (a) and shift number σ_{opt} (b) versus the interelement distance d for different apertures $(N = 58, 148, 293, 1354)$.

the d value does not only modify the visible range, but also breaks the symmetry of the power pattern with respect to the axis at $d \times u = \pm 0.5$. For illustrative purposes, Fig. 7 shows the plots of power patterns related to $\sigma_{opt}|_{d=0.5}$ [Fig. 7(a)] and $\sigma_{opt}^{MC}|_{d=0.5}$ [Fig. 7(b)] for different values of d.

As expected, a similar behavior of σ_{opt}^{MC} still verifies when varying the array aperture as shown in Fig. 8(a) for a thinning $\nu = 0.5$. Moreover, Fig. 8(b) further confirms that the PSL of an ideal array is usually smaller than PSL_{opt}^{MC} except for a limited range, whose upper threshold dth turns out to be inversely proportional to the number of lattice locations N [Fig. 8(b)]. Likewise the previous experiment, a ψ value greater (smaller) than ≈ 2.0 corresponds to the condition $\Delta > 0$ ($\Delta < 0$) [Fig. 9 — $d = 0.25$].

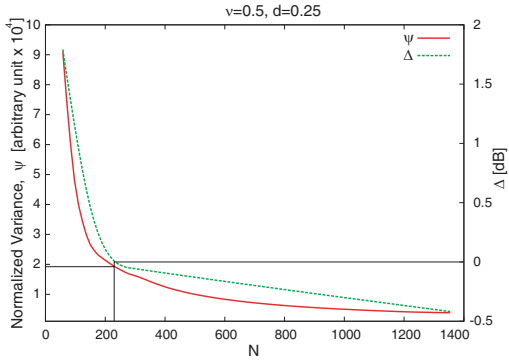

Figure 9. [$d = 0.25$, $\nu = 0.5$] — Normalized variance Ψ and Δ value versus N.

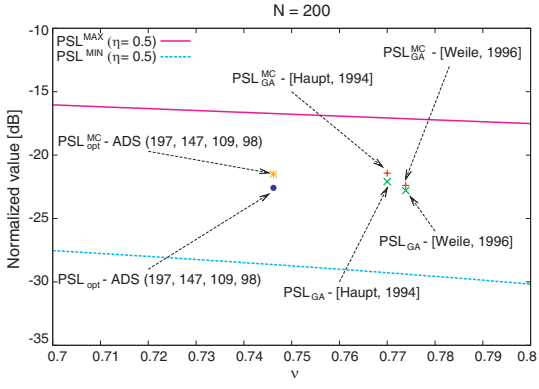

Figure 10. *Comparative Analysis* [$N \approx 200$] — PSL performances of GA-based arrays and ADS arrangements.

Table 1. *Comparative Analysis* — PSL values from DS-based and ADS-based arrays.

	N	ν	PSL_{opt} [dB]	PSL_{opt}^{MC} [dB]
DS	197	≈ 0.25	-13.22	-12.91
	107	≈ 0.5	-16.61	-15.81
	197	≈ 0.75	-22.96	-22.19
ADS	197	≈ 0.25	-13.56	-12.79
	107	≈ 0.5	-15.95	-15.23
	197	≈ 0.75	-22.57	-21.83

Finally, the last experiments are devoted to analyze the impact of MC effects on ADS-based arrays and state-of-the-art thinning techniques. First, a comparison with stochastic techniques is dealt with. Towards this end, a benchmark arrangement of $N = 200$ elements is considered. Fig. 10 shows the peak sidelobe levels synthesized with GA-optimized thinned arrays [5, 27] with and without MC as well as the corresponding values obtained with similar ADSs arrays [20]. The ideal ADS bounds when $\eta \triangleq \frac{t}{N-1} = 0.5$ are also reported. As it can be observed, the ADS-based arrays favourably compare with state-of-the-art GA designs despite the slightly smaller aperture (197 vs. 200) and thinning factor[‡]. Moreover, it worth noticing that the impact of MC more significantly affects their PSL ($\delta_{ADS} = -1.08$ vs. $\delta_{GA}^{[Haupt,\,1994]} = -0.67$ and $\delta_{GA}^{[Weile,\,1996]} = -0.40$) because of the "regularity" of ADS locations.

As far as the comparison with DSs is concerned, the results summarized in Tab. 1 indicate a greater robustness to mutual coupling effects of ADS designs compared to DS arrays ($\delta_{ADS}|_{\nu\approx 0.5} = -0.72$ vs. $\delta_{DS}|_{\nu\approx 0.5} = -0.80$ and $\delta_{ADS}|_{\nu\approx 0.75} = -0.74$ vs. $\delta_{DS}|_{\nu\approx 0.75} = -0.77$), except for very highly thinned arrays ($\delta_{ADS}|_{\nu\approx 0.25} = -0.77$ vs. $\delta_{DS}|_{\nu\approx 0.25} = -0.31$). Such a positive feature (although quite reduced, as it can be noticed from Table 1) is probably due to the enlarged number of degrees of freedom of ADS sequences and related autocorrelation functions [23].

[‡] Some research activities in the framework of combinatorial mathematics (out-of-the-scope of the present paper as well as of the focus of the *PIER Publications*.) are currently devoted to complete the set of ADS sequences in explicit form and, when available, they will allow a more fair comparison.

4. CONCLUSION

In this paper, the validity of PSL bounds deduced in [23] for ideal ADS arrays has been assessed in the presence of mutual coupling effects. An extensive numerical analysis has been carried out to evaluate the PSL performances of ADS arrangements in correspondence with different lattice spacings, thinning factors, and aperture dimensions. Representative results have been also provided in order to compare the sensitivity to MC of ADS-based thinned arrays with that of state-of-the-art approaches such as DS thinning and stochastically-optimized techniques. Such an analysis has pointed out that

- the values of PSL of ADS-based arrays in the presence of MC comply with the ideal bounds in [23] whatever the thinning value (Fig. 1), the array aperture (Fig. 1), and the lattice spacing [Fig. 5(a) and Fig. 8(a)];
- the differences between PSL_{opt}^{MC} and PSL_{opt} are more significant when d_{av} reduces [Fig. 2(f) and Fig. 3(f)]. In such a case, the optimal shift of the generating ADS sequence changes when the MC is present ($\sigma_{opt} \neq \sigma_{opt}^{MC}$) [Fig. 2(c) and Fig. 3(c)]. Otherwise, $PSL_{opt}^{MC} \approx PSL_{opt}$ [Fig. 2(a) and Fig. 3(a)] and $\sigma_{opt} = \sigma_{opt}^{MC}$ [Fig. 2(d) and Fig. 3(d)];
- a larger number of evaluations might be necessary to find the optimal shift σ_{opt}^{MC} when the MC is not negligible, although this number still remains below N [Fig. 4].

REFERENCES

1. Balanis, C. A., *Antenna Theory: Analysis and Design*, Wiley, New York, 1997.
2. Haupt, R. L. and D. H. Werner, *Genetic Algorithms in Electromagnetics*, Wiley, Hoboken, NJ, 2007.
3. Lo, Y. T., "A mathematical theory of antenna arrays with randomly spaced elements," *IEEE Trans. Antennas Propag.*, Vol. 12, No. 3, 257–268, May 1964.
4. Steinberg, B., "Comparison between the peak sidelobe of the random array and algorithmically designed aperiodic arrays," *IEEE Trans. Antennas Propag.*, Vol. 21, No. 3, 366–370, May 1973.
5. Haupt, R. L., "Thinned arrays using genetic algorithms," *IEEE Trans. Antennas Propag.*, Vol. 42, No. 7, 993–999, Jul. 1994.

6. Lommi, A., A. Massa, E. Storti, and A. Trucco, "Side lobe reduction in sparse linear arrays by genetic algorithms," *Microwave and Optical Technology Letters*, Vol. 32, No. 3, 194–196, 2002.
7. Caorsi, S., A. Lommi, A. Massa, S. Piffer, and A. Trucco, "Planar antenna array design with a multi-purpose GA-based procedure," *Microwave and Optical Technology Letters* Vol. 35, No. 6, 428–430, Dec. 20, 2002.
8. Caorsi, S., A. Lommi, A. Massa, and M. Pastorino, "Peak sidelobe reduction with a hybrid approach based on GAs and difference sets," *IEEE Trans. Antennas Propag.*, Vol. 52, No. 4, 1116–1121, Apr. 2004.
9. Donelli, M., S. Caorsi, F. De Natale, M. Pastorino, and A. Massa, "Linear antenna synthesis with a hybrid genetic algorithm," *Progress In Electromagnetic Research*, PIER 49, 1–22, 2004.
10. Massa, A., M. Donelli, F. De Natale, S. Caorsi, and A. Lommi, "Planar antenna array control with genetic algorithms and adaptive array theory," *IEEE Trans. Antennas Propag.*, Vol. 52, No. 11, 2919–2924, Nov. 2004.
11. Donelli, M., S. Caorsi, F. De Natale, D. Franceschini, and A. Massa, "A versatile enhanced genetic algorithm for planar array design," *Journal of Electromagnetic Waves and Applications*, Vol. 18, No. 11, 1533–1548, 2004.
12. Mahanti, G. K., N. Pathak, and P. Mahanti, "Synthesis of thinned linear antenna arrays with fixed sidelobe level using real-coded genetic algorithm," *Progress In Electromagnetics Research*, PIER 75, 319–328, 2007.
13. Zhang, S., S.-X. Gong, Y. Guan, P.-F. Zhang, and Q. Gong, "A novel iga-edspso hybrid algorithm for the synthesis of sparse arrays," *Progress In Electromagnetics Research*, PIER 89, 121–134, 2009.
14. Trucco, A. and V. Murino, "Stochastic optimization of linear sparse arrays," *IEEE J. Ocean Eng.*, Vol. 24, No. 3, 2910–299, Jul. 1999.
15. Trucco, A., "Thinning and weighting of large planar arrays by simulated annealing," *IEEE Trans. Ultrason., Ferroelectr., Freq. Control*, Vol. 46, No. 2, 347–355, Mar. 1999.
16. Razavi, A. and K. Forooraghi, "Thinned arrays using pattern search algorithms," *Progress In Electromagnetics Research*, PIER 78, 61–71, 2008.
17. Lee, K. C. and J. Y. Jhang, "Application of particle swarm

algorithm to the optimization of unequally spaced antenna arrays," *Journal of Electromagnetic Waves and Applications*, Vol. 20, No. 14, 2001–2012, 2006.

18. Donelli, M., A. Martini, and A. Massa, "A hybrid approach based on PSO and Hadamard difference sets for the synthesis of square thinned arrays," *IEEE Trans. Antennas Propag.*, Vol. 57, No. 8, 2491–2495, Aug. 2009.
19. Leeper, D. G., "Isophoric arrays-massively thinned phased arrays with well-controlled sidelobes," *IEEE Trans. Antennas Propag.*, Vol. 47, No. 12, 1825–1835, Dec. 1999.
20. ELEDIA Almost Difference Set Repository, http://www.eledia.-ing.unitn.it/.
21. Kopilovich, L. E. and L. G. Sodin, "Linear non-equidistant antenna arrays based on difference sets," *Sov. J. Commun. Technol. Electron.*, Vol. 35, No. 7, 42–49, 1990.
22. Kopilovich, L. E. and L. G. Sodin, *Multielement System Design in Astronomy and Radio Science*, Kluwer Academic Publishers, Boston, 2001.
23. Oliveri, G., M. Donelli, and A. Massa, "Linear array thinning exploiting almost difference sets," *IEEE Trans. Antennas Propag.*, In press (available in the *IEEE-TAP Forthcoming Articles* at http://ieeexplore.ieee.org/xpl/tocpreprint.jsp?isnumber=4907023 &punumber=8).
24. Ding, C., T. Helleseth, and K. Y. Lam, "Several classes of binary sequences with three-level autocorrelation," *IEEE Trans. Inf. Theory*, Vol. 45, No. 7, 2606–2612, Nov. 1999.
25. Arasu, K. T., C. Ding, T. Helleseth, P. V. Kumar, and H. M. Martinsen, "Almost difference sets and their sequences with optimal autocorrelation," *IEEE Trans. Inf. Theory*, Vol. 47, No. 7, 2934–2943, Nov. 2001.
26. Huang, Z., C. A. Balanis, and C. R. Birtcher, "Mutual coupling compensation in UCAs: Simulations and experiment," *IEEE Trans. Antennas Propag.*, Vol. 54, No. 11, 3082–3086, Nov. 2006.
27. Weile, D. S. and E. Michielssen, "Integer-coded Pareto genetic algorithm design of antenna arrays," *Electron. Lett.*, Vol. 32, 1744–1745, 1996.
28. La Jolla Cyclic Difference Set Repository, http://www.ccrwest.org/diffsets.html.